CONF-771136-28

PREPRINT UCRL-79861

Lawrence Livermore Laboratory

X-RAY LINES AS A DENSITY DIAGNOSTIC IN DT PLASMAS NEAR 100X SOLID DENSITY

David S. Bailey

MASTER

October 19, 1977

This paper was prepared for presentation at the 19th Meeting of the American Physical Society/Division of Plasma Physics, Atlanta, Georgia, November 6-11, 1977.

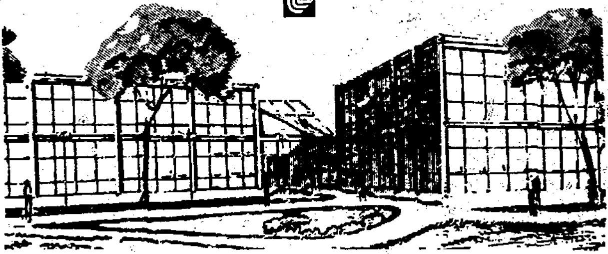

X-RAY LINES AS A DENSITY DIAGNOSTIC IN DT PLASMAS NEAR 100X SOLID DENSITY*

David S. Bailey

Lawrence Livermore Laboratory
University of California
Livermore, California 94550

ABSTRACT

The use of electron impact broadened resonance lines to diagnose near-term high density diagnostics is discussed. In particular, the question of how to choose seed and pusher materials to have discernible broadening effects while maintaining line visibility is discussed.

*Research performed under the auspices of the U.S. Energy Research and Development Administration under Contract No. W-7405-Eng-48.

Along the path to an ultimate laser fusion target that achieves densities of several thousand x liquid densities and few kilovolt temperatures, one is faced with achieving near isentropic implosions that give high densities but low temperatures. This combination makes diagnosing such targets very difficult - due to the low temperature not much radiation or yield is generated and because of the high density what there is tends to be reabsorbed before it escapes. It is the purpose of this paper to extend the line emission diagnostic first used in the LLL 10x liquid density experiments[1] to the 100x liquid density regime. The basis of the line calculations below is a post-processor code for LASNEX that has been described previously.[2]

The issues involved are summarized in Fig. 1 and amount to ensuring line visibility without perturbing the initial target designs unduly. The line intensity is most strongly affected by the temperature in the fuel region and the attenuation in the pusher before a line photon escapes suggests using a high Z seed and low Z pusher. In contrast, the sensitivity of the line width to density effects decreases with increasing Z, so a balance is required. Also, the choice of pusher material affects the implosion by changing the preheat, initial density, etc., so that the implosion in general is degraded and this loss must be minimized. These factors will now be discussed in detail.

A) Line intensity - In Fig. 2 is shown a simple model for the scaling of the line intensity and background continuum emission. Assuming a homogeneous fuel and pusher shell, the intensity ratio of line/background is determined by the temperature ratio and relative areas, with an extra loss due to shell attenuation of the line. The fundamental requirement is to have the core hotter than the pusher. For an ablative implosion this is normally the case, since the whole idea is to maximize the efficiency of energy transfer to the fuel region. Given this requirement, one has an exponential gain factor that must make up the losses due to shell attenuation of the line as well as its lower area of emission. The parameters chosen in the example are similar to those from sample implosions, and with a pusher attenuation of 2x or less (implying a low Z material) yield an overall line/background ratio of 5 or better for the lowest ($n = 2$) helium resonance line, which should provide visibility of three helium series members. As shown in Fig. 3, the limit to this scheme comes when the core region becomes thick in the continuum. Since this limit is *above an electron density of 10^{26} cm^{-3}(~ 3500x liquid density* in DT), it could still be used on breakeven targets.

B) Line Broadening - Fig. 4 shows the many components to the observed line width; we want to have the density component determine the observed width. As shown in Fig. 5, for the conditions appropriate here the fine structure splitting (important only for the lowest hydrogen resonance line) is comparable to the Doppler broadening and will in that case be essentially additive. On Fig. 6 are described the effects of electron impact and quasi-static ion broadening. For hydrogen, which due to degeneracy has a linear Stark effect, the ion broadening is so large that those components vanish below the continuum, and the remaining part is the electron broadened unshifted component. In the case of helium, with a quadratic Stark effect, the shift is too small for the $n = 2$

resonance line to notice, and becomes hydrogen-like for higher members. The helium $n = 2$ resonance line also has other features of lower intrinsic intensity, namely the plasma satellites and forbidden and intercombination lines that may be visible if the central component is opaque enough. The basic density mechanism used here is the electron broadening, and we want to ensure the density broadening dominates the line profile. In Fig. 7 we show the results of equating the Doppler width and impact width; this yields an upper bound for the Z of the seed material at any given electron density. To complete the discussion of the observed line profile, we must include (as on Fig. 8) the effects of opacity broadening and instrument resolution. To ensure seeing at least the $n = 2$ resonance line, we choose a seed fill pressure to achieve an optical depth of ~ 50 at the desired implosion conditions. This leads to an extra broadening of ~ 3x the intrinsic line width for a Lorentzian profile. Although this broadening does provide extra complications, the idea is that one is thereby guaranteed seeing at least the $n = 2$ line and can extract the intrinsic profile directly from the higher lines if they are visible. In the 2-3 keV region appropriate for these conditions, instrument resolutions of 2-3 eV are readily feasible, and should not be significant compared to the intrinsic width.

C) Experiment Design - In Fig. 9 are shown the parameters for a nominal 100x implosion appropriate to the LLL Argus laser in long pulse operation. The target design is discussed in more detail by W. Mead.[3] The changes from the initial (non-diagnostic) design include

1) longer laser pulse - slightly lower power
2) larger target - lower laser intensity, larger compressed radius, and longer time in compressed state.

The net result of these changes was to raise the line/background ratio (for both P and Ar) by an order of magnitude (mainly due to the increased core radius) with a loss of 2x in the final density achieved. On the basis of the previous discussion of the scaling for line widths, since the phosphorus (Z = 15) has three resonance lines visible, it is preferable as a seed for a density diagnostic. As a practical matter, it is probably much easier to fill with argon (Z = 18) and as shown in Fig. 10, Ar also has three resonance lines above the continuum, it will also suffice; particularly if the higher lines are seen.

In summary, we have discussed the scaling rules for seed and pusher materials to use for diagnosing cold, dense implosions. This scheme is possible to beyond 1000x liquid density implosions, and at the 100x level incurs only modest penalties in achieved density and extra fabrication difficulty.

REFERENCES

1. J. M. Auerbach et al., Lawrence Livermore Laboratory Report UCRL-79636, June, 1977.

2. D. S. Bailey and E. J. Valeo, Lawrence Livermore Laboratory Report UCRL-78473, 1976.

3. W. Mead, Lawrence Livermore Laboratory Report UCRL-79733, 1977.

FACTORS AFFECTING MATERIAL CHOICES FOR A SUCCESSFUL DIAGNOSTIC

- LINE VISIBILITY – WANT HIGH CONTRAST TO BACKGROUND AND GREATER THAN MINIMUM INSTRUMENT SENSITIVITY.

  ⇒ PICK Z OF SEED TO SET $E_L/T_e \sim 5$

  LOW Z PUSHER DECREASES SHELL ATTENUATION AND BACKGROUND EMISSION

- LINE BROADENING – DENSITY COMPONENT OF INTRINSIC LINE WIDTH SHOULD BE DOMINANT

  ⇒ USE LOWEST Z SEED POSSIBLE

  UTILIZE HIGHER SERIES MEMBERS (LOWER OPACITY EFFECT, HIGHER DENSITY SENSITIVITY)

- MATCH TO TARGET DESIGN – MINIMIZE DEGRADATION ON TARGET FROM DIAGNOSTIC MODIFICATIONS (PRE-HEAT, ETC.)

Fig. 1

LINE VISIBILITY

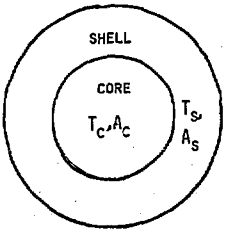

ASSUMING BLACK-BODY SATURATION,

$$\frac{I_c}{I_s} = \frac{A_c}{A_s} \cdot \frac{e^{-E_L/T_c}}{e^{-E_L/T_s}} \cdot F_{EXT}$$

F_{EXT} — SHELL ATTENUATION OF LINE

$$\frac{I_c}{I_s} = \left(\frac{A_c}{A_s} \cdot F_{EXT}\right) e^{\frac{E_L}{T_c}\left(\frac{T_c}{T_s} - 1\right)}$$

$\left(\frac{A_c}{A_s} \cdot F_{EXT}\right)$ — LOSSES; exponential — GAIN FACTOR

EXAMPLE: $E_L/T_c = 5$, $T_c/T_s = 2$

⇒ GAIN FACTOR OF 150x

$\frac{A_c}{A_s} \sim \frac{1}{10}$, NOT ADJUSTABLE

F_{EXT} DEPENDS ON Z OF PUSHER (GENERALLY NEAREST K-EDGE)

⇒ BETTER AT LOW Z

Fig. 2

LINE VISIBILITY

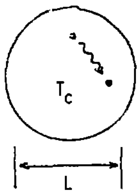

ULTIMATE LIMIT COMES WHEN CONTINUUM BECOMES THICK IN CORE AND BLANKETS LINE:

$$K_\nu = \frac{4}{3}\left(\frac{2\pi}{3mkT_c}\right)^{1/2}\frac{Z^2 e^6}{hcm\nu^3}\quad N_i N_e$$

$$= 7.7 \times 10^{-52}\, Z^2\, \frac{N_i N_e}{T_c^{3/2}\, x^3}\quad \mu m^{-1}\quad \begin{cases} x = E_L/T_c \\ T_c \text{ in keV} \end{cases}$$

FOR $Z = 1$, $x = 5$, $L = 5\,\mu m$, $T_c = 1$ keV

$K_\nu L = 1 \Rightarrow N_e \lesssim 2 \times 10^{26}$ cm^{-3} (835 g/cm^3 for DT or 4000x liquid)

Fig. 3

THE OBSERVED LINE IS A COMBINATION OF VARIOUS BROADENING EFFECTS

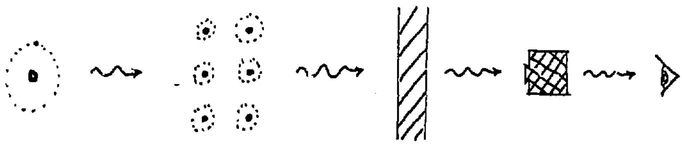

ATOMIC EFFECTS — FINE STRUCTURE, DOPPLER, STARK

OPACITY BROADENING

SHELL ATTENUATION

SPECTROMETER RESOLUTION

OBSERVABLE LINE

Fig. 4

LINE BROADENING SOURCES

A) FINE STRUCTURE SPLITTING. SPLITS HYDROGENIC INTRINSIC WIDTH INTO TWO COMPONENTS SEPARATED BY $3.62 \times 10^{-4} \frac{Z^4}{n^3}$ eV (2.3 eV FOR P $L_\gamma \alpha$)

B) DOPPLER BROADENING.

1) ION TEMPERATURE

(A) GIVES GAUSSIAN SHAPE;

(B) $\omega_D \cong .021\, Z^{1.5} \sqrt{T_i}$ (eV)

2) DIRECTED MASS MOTION

(A) IMPLOSION PHASE VELOCITIES $\lesssim 10^7$ cm/sec, CORRESPONDING TO ~ 1 eV;

(B) HOWEVER DENSITY LOW, EXPECT SMALL EFFECT.

Fig. 5

LINE BROADENING - (CONTINUED)

C) STARK BROADENING

1) QUASI-STATIC ION BACKGROUND - PRODUCES WINGS 13-50 eV WIDE.

2) ELECTRON COLLISIONS

$$\omega_S = 6.9 \times 10^{-24} \cdot \frac{n^4}{Z^2} \cdot \frac{N_E}{\sqrt{T_E}} \text{ (eV)}$$

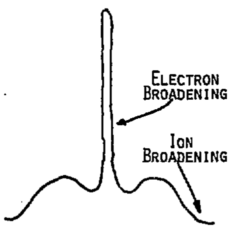

3) INTENSITY TOO LOW TO SEE ION WINGS.

4) THIS WIDTH MAY BE FACTOR OF 2 TOO LOW (FOR HYDROGEN)

(A) HIGH-DENSITY EXPERIMENTS INDICATE ERROR IN CLASSICAL THEORY

(B) GRIEM POSTULATES ADDITIONAL WIDTH DUE TO ION PLASMA FREQUENCY PERTURBATION.

Fig. 6

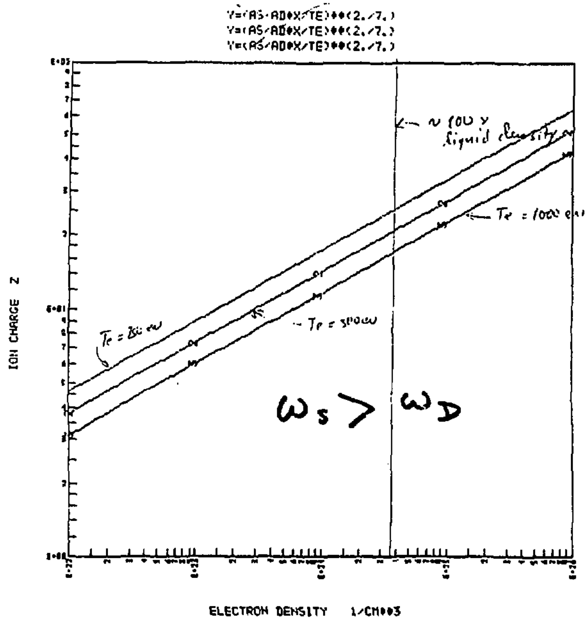

Fig. 7

LINE BROADENING - (CONTINUED)

D) OPTICAL TRANSFER EFFECTS

(1) LINE PROFILE IS PROPORTIONAL TO PROBABILITY OF PHOTON ABSORPTION, EMISSION.

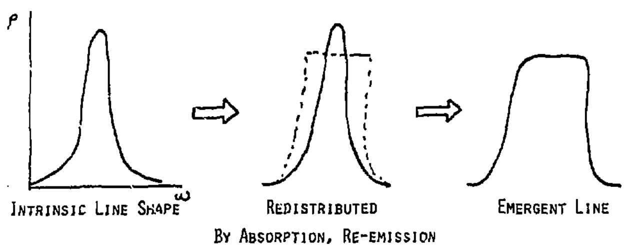

E) SPECTROMETER INSTRUMENTAL RESOLUTION

EMERGENT LINE FURTHER CONVOLUTED WITH INSTRUMENT TRANSFER FUNCTION

Fig. 8

EXPERIMENT DESIGNED TO DIAGNOSE HIGH DENSITY COMPRESSION

- GOALS: DENSITY $\gtrsim$ 20 G/CM^3
  ELECTRON TEMPERATURE $\simeq$ 550 eV
  LINE/BACKGROUND INTENSITY HIGH

- METHOD: (1) SLOW LASER PULSE
  (2) LARGE DIAMETER, THICK WALLED PELLET
  (3) LOW Z PUSHER

- EXPERIMENTAL PARAMETERS: (1) 2500 J IN 1 NS
  (2) 150 μM (INNER) DIAMETER BALL, 20 μM WALL
  (3) PUSHER MATERIAL IS BE (Z = 4)
  (4) LASNEX RESULTS: ρ_{MAX} = 12 G/CM^3, TE = .53 KEV
  WITH LINE/BACK = { 6 P (~2 KEV) ; 8 AR (~3 KEV) }

Fig. 9

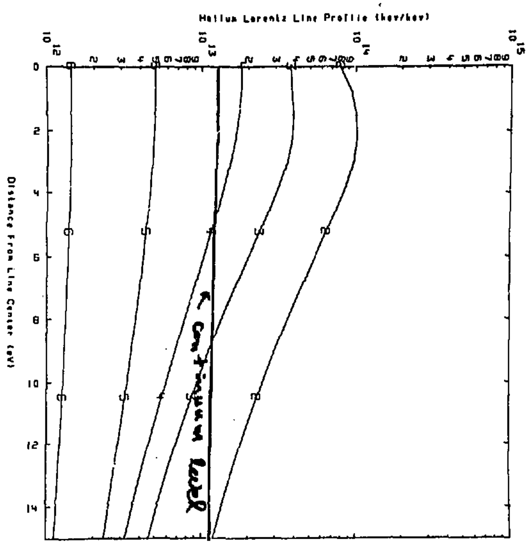

Fig. 10